

Simulation and measurement of short infrared pulses on silicon position sensitive device

This content has been downloaded from IOPscience. Please scroll down to see the full text.

2011 JINST 6 C01036

(<http://iopscience.iop.org/1748-0221/6/01/C01036>)

View [the table of contents for this issue](#), or go to the [journal homepage](#) for more

Download details:

IP Address: 145.101.41.118

This content was downloaded on 06/02/2017 at 11:08

Please note that [terms and conditions apply](#).

You may also be interested in:

[Particle detectors based on semiconducting InP epitaxial layers](#)

R Yatskiv, J Grym and K Zdansky

[ATLAS silicon microstrip detector operation and performance](#)

E Coniavitis

[In situ analysis of carrier lifetime and barrier capacitance variations in silicon during 1.5 MeV protons implantation](#)

T Ceponis, E Gaubas, V Kalendra et al.

[Study of X-ray radiation damage in silicon sensors](#)

J Zhang, E Fretwurst, R Klanner et al.

[Design of pixel electronics based on asynchronous self-reset approach with floating-point output representation for high dynamic range imagers](#)

A Nascetti and P Valerio

[SiC X-ray detectors for harsh environments](#)

J E Lees, A M Barnett, D J Bassford et al.

[Pixel sensitivity variations in a CdTe-Medipix2 detector using poly-energetic x-rays](#)

R Aamir, S P Lansley, R Zainon et al.

[Material reconstruction with the Medipix2 detector with CdTe sensor](#)

E Guni, J Durst, T Michel et al.

[Suppression of irradiation effects in gold-doped silicon detectors](#)

M McPherson, T Sloan and B K Jones

12th INTERNATIONAL WORKSHOP ON RADIATION IMAGING DETECTORS,
JULY 11th–15th 2010,
ROBINSON COLLEGE, CAMBRIDGE U.K.

Simulation and measurement of short infrared pulses on silicon position sensitive device

D. Krapohl,¹ O.X. Esebamen, H.E. Nilsson and G. Thungström

^a*Department of Information Technology and Media,
Holmgatan 10 85170 Sundsvall, Sweden*

E-mail: david.krapohl@miun.se

ABSTRACT: Lateral position sensitive devices (PSD) are important for triangulation, alignment and surface measurements as well as for angle measurements. Large PSDs show a delay on rising and falling edges when irradiated with near infra-red light [1]. This delay is also dependent on the spot position relative to the electrodes. It is however desirable in most applications to have a fast response. We investigated the responsiveness of a Sitek PSD in a mixed mode simulation of a two dimensional full sized detector. For simulation and measurement purposes focused light pulses with a wavelength of 850 nm, duration of 1 μ s and spot size of 280 μ m were used. The cause for the slopes of rise and fall time is due to time constants of the device capacitance as well as the photo-generation mechanism itself [1]. To support the simulated results, we conducted measurements of rise and fall times on a physical device. Additionally, we quantified the homogeneity of the device by repositioning a spot of light from a pulsed ir-laser diode on the surface area.

KEYWORDS: Solid state detectors; Detector modelling and simulations II (electric fields, charge transport, multiplication and induction, pulse formation, electron emission, etc); Photon detectors for UV, visible and IR photons (solid-state)

¹Corresponding author.

Contents

1	Introduction	1
2	Simulation	1
3	Measurements	2
4	Results	3
5	Conclusion	4

1 Introduction

The current response to an applied light pulse in a position sensitive device shows a time delay due to the device's high resistivity and capacitance. A device with a low surface resistivity allows for quicker responses and less distorted current pulses.

This paper describes the simulation of such a device. A $1\text{ }\mu\text{m}$ slice of the PSD is simulated in a Medici simulation using pulses of light. Two different reverse bias levels were applied as well as three different infra-red wavelengths. The simulation results are compared with measurements conducted on the physical device.

2 Simulation

A slice of the PSD was modelled in two dimensions using four contacts, two placed on the top edge and two on the bottom. In this way it was possible to approximate the original device which has the bottom pair of contacts rotated by 90 degrees. The dimensions of the slice on the y and x-axis are $12200\text{ }\mu\text{m} \times 380\text{ }\mu\text{m}$ respectively, this corresponds to the dimensions of the real detector as shown in figure 1. The slice has a standard thickness of $1\text{ }\mu\text{m}$.

The TCAD model was created in MEDICI, a mixed mode device circuit simulator, by describing the dimensions and importing doping profiles [2]. These profiles were extracted from a simulated implantation process, simulated with SENTAUROS SPROCESS, using values provided by the vendor [3]. In order to achieve the desired resistivity of $1.2\text{ k}\Omega$ between the top contacts and $1.3\text{ k}\Omega$ between the bottom contacts, two doping profiles were used, one along the top edge and a second along the bottom. A reverse bias of 15 V and 30 V was applied during the simulation to create a depletion capacitance matching measurement results.

Meshing was done in two steps. An initial mesh with very coarse spacing in the centre of the device was applied. The mesh geometry was then refined in order to correspond to the concentration of atoms in the doping profile, resulting in a finer mesh along the edges of the detector as shown in figure 1. The general meshing strategy was to define as many mesh points as possible

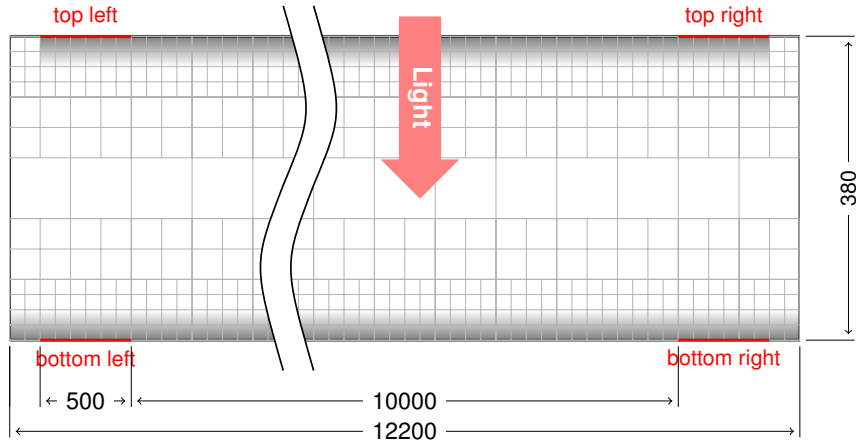


Figure 1. Sketch of simulated device structure. Contacts are drawn in red along the top and bottom surface. The mesh is stylized in light grey boxes with finer structures towards the faded regions depicting the doped areas. All numbers are in micro meters.

while staying below the 60000 elements limit of MEDICI. Mobility models considering parallel electric field component and impurity concentration as well as Shockley-Read-Hall recombination using fixed lifetimes in two steps, $0.5 \mu\text{s}$ and $0.6 \mu\text{s}$, were enabled in all simulations.

We ran each model for wavelengths of 850 nm, 980 nm and 1060 nm, each with updated optical properties [4]. Two light spot positions were simulated, one at the centre of the device and the second 2.5 mm to the right of the first. Each position was simulated with 15 V and 30 V reverse bias. A transient simulation was run with time steps of about 1 ns for an overall duration of $1.5 \mu\text{s}$ insuring that the tail of the current pulse was included. The virtual device contained about 54929 triangular mesh elements having an execution time of about 3 hours for each simulation on a single Xeleron core (2.4 GHz).

The data from MEDICI was logged into a standard IC-CAP data file that was later analysed using a file reader and scripts written in Scientific Python [5]. The simulated data was interpolated with about 10000 equally distributed steps in order to simplify automatic extraction of current levels and rise and fall time calculations. To find the 10% and 90% threshold levels of the signal, an average of 50 data points around the minimum and maximum current levels were calculated.

3 Measurements

The rise and fall time measurements were performed by connecting the two top contacts of the PSD directly to a Tektronix 11302 oscilloscope featuring a 11052A plug-in with 50Ω input resistance, thus avoiding any other parasitic capacitances or amplifiers (see figure 2). 15 V or 30 V reverse bias was connected to the bottom contacts. Two VCSEL laser diodes (Finisar HFE4192-5810, Thorlabs VCSEL-980) with centre wavelengths of 850 nm and 980 nm and a maximum rise time of 100 ps were used to emit light pulses. The laser diode and series resistance was terminated with a 50Ω resistor and directly connected to a function generator (HP 8116A) as shown in figure 2. The laser diode was coupled to an optical fibre in order to focus the light onto the centre of the PSD. With the aid of a power meter (Thorlabs, PM100D), the average output power of the focused beam was

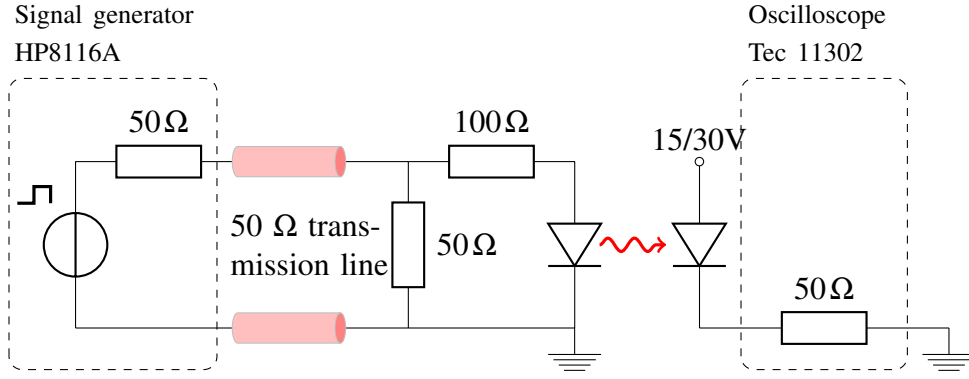


Figure 2. Schematic of the measurement set-up. The left side shows the circuit driving the laser diode, the right part of the graph the measurement circuit containing the PSD connected to the oscilloscope.

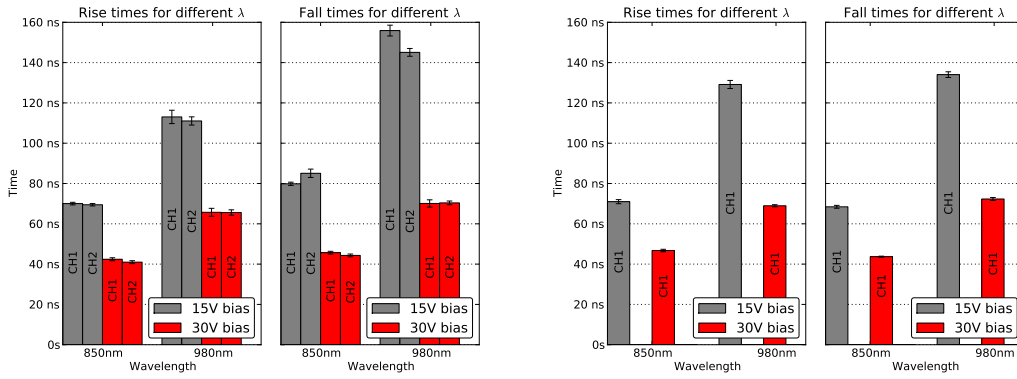


Figure 3. The graphs to the left show measurement results for the two top terminals (CH1,CH2) using wavelengths of 850 nm and 980 nm as well as 15 V and 30 V reverse bias. The plots on the right show measurements from one terminal (closer to the light spot) with the spot of light moved 2.5 mm towards the contact.

adjusted to 120 mW. For every reverse bias voltage an average of five measurements was taken for each contact. The rise times of the oscilloscope and function generator were then taken into account and the data adjusted accordingly using the following equation

$$t_r = \sqrt{t_{\text{tot}}^2 - t_{\text{osc}}^2 - t_{\text{func}}^2} \quad (3.1)$$

with time constants of $t_{\text{func}} = 6 \text{ ns}$, $t_{\text{osc}} = 2 \text{ ns}$ of function generator and oscilloscope, respectively.

4 Results

The simulated device has a calculated depletion width of 139.2 μm and 97.5 μm for 30 V and 15 V respectively. This results in a capacitance of 75.7 pF/cm² and 108 pF/cm² [6].

With longer wavelengths a considerable amount of electron-hole pairs are generated below the depletion region. Using the Beer-Lambert law for absorption $I = I_0 \cdot \exp(-\alpha \cdot x)$, it can be shown through calculation that for longer wavelengths more of the radiation penetrates deeply the

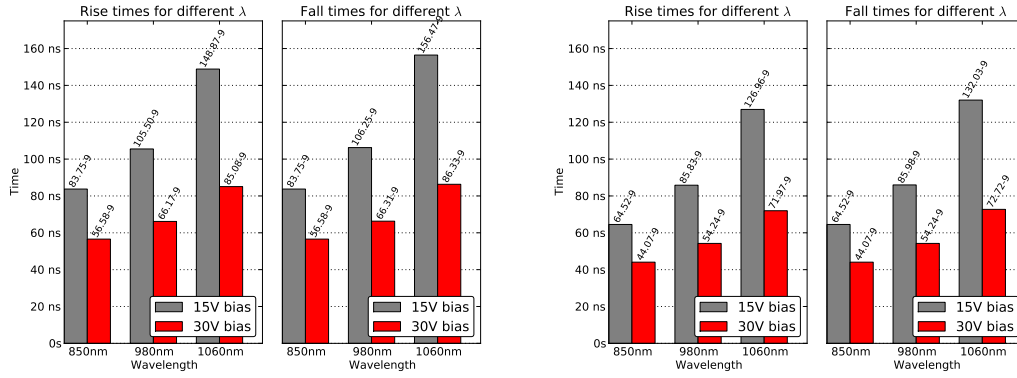


Figure 4. The graphs show simulation results for three different wavelengths and reverse bias. The left graphs show results with a centred light pulse. The right graphs show results from simulations with a light spot 2.5 mm moved to the right and the contact closest to the spot.

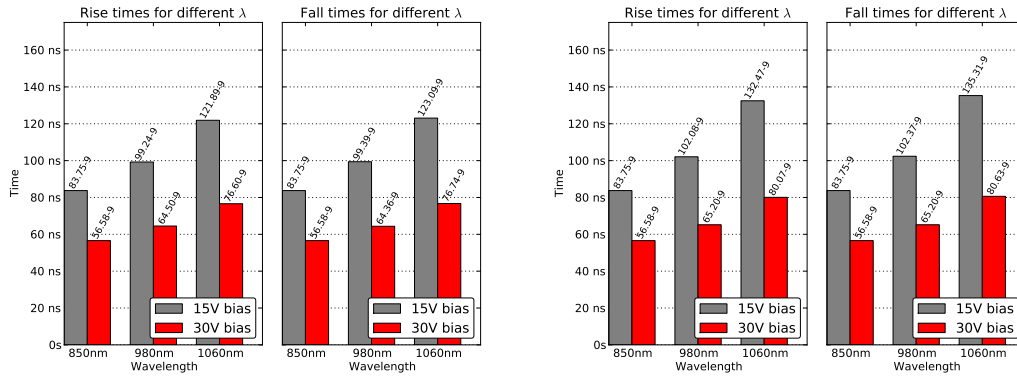


Figure 5. The left graphs show results for simulations done with a electron-hole life time set to $\tau_{n/p}=0.4 \mu\text{s}$. The right graph shows results for simulations done with a electron-hole life time set to $\tau_{n/p}=0.5 \mu\text{s}$.

depletion region due to a lower absorption coefficient. Thus, rise and fall times become longer as more electron-hole-pairs are generated below the depletion length and extend the diffusion time. Extending the lifetime of charge carriers results in longer raise and fall time particularly for longer wavelengths. As opposed to pure RC-circuit simulation done by Kreisler et. al., a mixed signal simulation reveals the influence of charge carrier lifetime [7]. The values found with lifetime of $\tau_{n/p} = 0.65 \mu\text{s}$ (see figure 4) are close to those obtained from measurements on the physical device shown in figure 3. From figure 5 it can be seen that not all charges are collected when $\tau_{n/p}$ is set to $0.4 \mu\text{s}$ or $0.5 \mu\text{s}$, respectively. These results show that one cannot neglect the influence of the diode itself and simply simulate the distributed RC-components.

5 Conclusion

Simulation and measurements show very similar results with adjusted charge carrier lifetime of $\tau_{n/p} = 0.6 \mu\text{s}$. As expected, rise and fall times with lower reverse bias are longer because of a

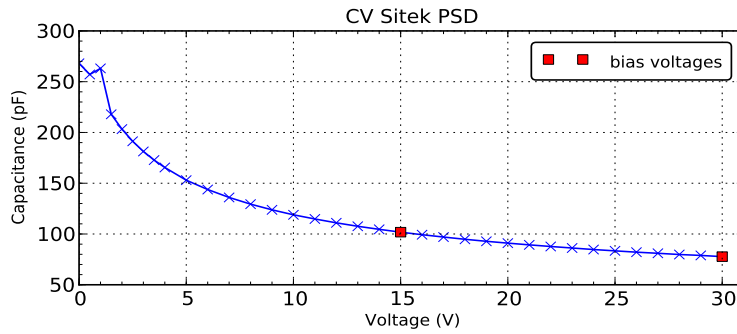


Figure 6. The CV graph of measurement results on the position sensitive device. The two top terminals and bottom terminals were connected at a time. The two selected reverse bias voltages are marked with red squares.

lower depletion length and therefore a higher influence of charge diffusion. At 30 V reverse bias the device has a fast response despite its large active area because of its low surface resistance and capacitance (see figure 6).

Since the device is not fully depleted, electron hole pairs generated in deeper regions are collected much slower than those generated in the depleted region. This becomes more obvious at longer wavelengths when more photo-generation takes place in deeper regions of the device. It is therefore important to take electron hole recombination into account which can only be provided by a mixed signal simulation rather than a simple RC-equivalent circuit simulation.

Acknowledgments

We would like to thank the company Sitek AB for their support and for kindly providing the position sensitive device.

References

- [1] M.D. Bakker et al., *The PSD transfer function*, *IEEE T. Electron Dev.* **49** (2002) 202.
- [2] *Taurus Medici user guide*, D-2010.03, (2010).
- [3] *Sentaurus process user guide*, D-2010.03, (2010).
- [4] M.A. Green and M.J. Keevers, *Optical properties of intrinsic silicon at 300K*, *Prog. Photovoltaics* **3** (1995) 189.
- [5] E. Jones, T. Oliphant and P. Peterson, *SciPy: open source scientific tools for Python*, (2001).
- [6] S.M. Sze and K.K. Ng, *Physics of semiconductor devices*, Wiley, U.S.A. (2007).
- [7] C. Klein and R. Bierig, *Pulse-response characteristics of position-sensitive photodetectors*, *IEEE T. Electron Dev.* **21** (1974) 532.